Journal of Alloys and Compounds 587 (2014) 153–157

Contents lists available at ScienceDirect

Journal of Alloys and Compounds

journal homepage: www.elsevier.com/locate/jalcom

Characterization of temperature-dependent photoluminescence properties of InAlGaN quaternary alloys

S.Y. Hu [a,*], Y.C. Lee [b], Y.H. Weng [c], I.T. Ferguson [d], Z.C. Feng [e]

[a] Department of Digital Technology Design, Tungfang Design Institute, Hunei, Kaohsiung 82941, Taiwan
[b] Department of Electronic Engineering, Tungnan University, Shenkeng, New Taipei 22202, Taiwan
[c] Department of Electrical Engineering, National Taiwan Ocean University, Keelung 20224, Taiwan
[d] Department of Electrical and Computer Engineering, University of North Carolina at Charlotte, Charlotte, NC 28223, USA
[e] Institute of Photonics and Optoelectronics, Department of Electrical Engineering, Center for Emerging Material and Advanced Devices, National Taiwan University, Taipei 10617, Taiwan

ARTICLE INFO

Article history:
Received 2 August 2013
Received in revised form 15 October 2013
Accepted 17 October 2013
Available online 30 October 2013

Keywords:
InAlGaN alloy
Photoluminescence
X-ray diffraction
Stress

ABSTRACT

Samples containing thin InAlGaN layers grown on c-Al_2O_3 substrates by metalorganic chemical vapor deposition have been studied experimentally and theoretically with the help of photoluminescence measurements between 10 and 300 K. From the analysis of the temperature dependence photoluminescence spectra with the modified Bose–Einstein equation, the localization energy of excitons was estimated successfully and the value is found out to be well correlated to the strength of the electron/exciton-phonon interaction as well as the stress observed in the X-ray diffraction spectra. These results are also confirmed that the c-axis length decreases as the increasing Al/In ratio corresponding to the decreased compressive stress which would be attributed to the increased tensile stress formed by Al atoms incorporated.

1. Introduction

III-nitride based alloys have been extensively studied for the understanding of fundamental physics to improve the achievement in the optical fields such as deep ultraviolet (UV) light emitting diodes (LEDs) and white light LEDs [1–3]. For optical device applications, high-quality emission properties are essential so it is quite important to carry out better optical properties of these nitride-based alloys. Generally, in the quaternary alloy system, atoms of the constituent binary or ternary semiconductors are randomly distributed, leading to fluctuations in masses and force constants in the neighborhood, which is known as the alloying effect. In particular, it has been found that incorporating a small amount of indium (In) into AlGaN can overcome those drawbacks of ternary alloys [4–7]. Then, InAlGaN alloys have been regarded as the most promising candidates to replace ternary alloys of InGaN or AlGaN due to their band gap, lattice constant, and thermal properties that can be independently adjusted by varying either indium (In) or aluminum (Al) compositions [4–7]. Although there are already some reports on optical investigations of quaternary InAlGaN systems, the physical origins of the emission spectra being utilized for light emission components are not yet fully understood [6–8]. Further improvements in the material quality of this quaternary alloy system are still necessary. Consequently, there comes out a demand for a comprehensive study on the properties of the optical transitions and their dynamic processes in InAlGaN layers, which could provide not only a better understanding of fundamental optical properties, but also provide input for potential approaches toward the better materials quality as well as the design of specific device structures.

In this work, we present a study of one set quaternary InAlGaN samples by means of the temperature dependence photoluminescence (PL) measurements in the range of 10–300 K to concern with the determination of the energy characteristics that specifies the relationship between localization energy and stress in the InAlGaN quaternary alloys.

2. Experimental

One set of quaternary $In_xAl_yGa_{1-x-y}N$ alloys used in this work were produced by low pressure metalorganic chemical vapor deposition (MOCVD). Each structure of the samples consists of one GaN layer, about 1 μm, grown on the c-Al_2O_3 substrate, followed by a low temperature 25 nm AlN buffer layer and 230 nm of $In_xAl_yGa_{1-x-y}N$. Further growth procedures are described elsewhere [9]. X-ray photoelectron spectroscopy (XPS) was employed to estimate the chemical composition of Al (aluminum) to be 13.97% for M14, 10.52% for M12, and 31.50% for M04, respectively, while In (indium) to be 2.73% for M14, 1.38% for M12, and 3.50% for M04, respectively. Then, we can find the Al/In to be 5.1 for M14, 7.6 for M12, and 9.0 for M04, respectively. The photoluminescence spectra of the quaternary InAlGaN samples were measured from 10 to 300 K by using a 5 mW/cm^2 microchip

* Corresponding author. Tel.: +886 7 6939632x102; fax: +886 7 6932348.
E-mail addresses: shenghu2729@yahoo.com (S.Y. Hu), zcfeng@ntu.edu.tw (Z.C. Feng).

0925-8388/$ - see front matter © 2013 Elsevier B.V. All rights reserved.
http://dx.doi.org/10.1016/j.jallcom.2013.10.139

(λ = 266 nm) laser as the excitation source inside a closed-cycle He cryostat with a modified and computer controlled LakeShore 321 model temperature controller under an accuracy of ±0.5 K. The photoluminescence was analyzed by using a monochromator (Acton SP-2150i) with a 1200 grooves/mm grating and detected using a cooled GaAs photomultiplier tube. The structural properties of the InAlGaN quaternary samples were analyzed by high resolution X-ray diffraction (HRXRD).

3. Results and discussion

Measurements of the PL spectra for the three quaternary InAlGaN samples, namely M14, M12, and M04 as labeled in Fig. 1a for 10 K and Fig. 1b for 300 K, respectively were made under the same excitation conditions. As shown in Fig. 1b, the short-wavelength PL signal has been previously assigned to be the InAlGaN-based transition, and the GaN-related features appearing on the right side of the InAlGaN-based PL peaks are all just about located at 364 nm for the samples of M14 and M12, respectively [8,10]. However, it is also observed that the InAlGaN-based PL peaks of M12 and M04 are quite stronger while the InAlGaN-based PL peak is very weak for M14, probably it is due to the lattice-matched ratio between Al and In which is close to 4.7 [11]. Here, we focus on the comparison of the InAlGaN-based PL emission properties and the PL emission bands have been attributed to a recombination of localized excitons, as often observed in the nitride-based semiconductor alloys [12–15].

In our work, the typical PL spectra of sample M12 at several different temperatures from 10 to 300 K is shown in Fig. 2a, while the PL peak position (opened circles) as a function of temperature is shown in Fig. 2b. From the temperature dependence results in Fig. 2b, it is observed that the InAlGaN epilayers differ from the usual semiconductor temperature-dependent band gap shrinkage behavior. In sample M14, above/below ~30 K, the PL peak position displays S-shaped phenomena, which provide evidence of exciton localization in potential minima caused by alloy fluctuations [1,13,14]. Similar temperature dependence were observed in samples M12 and M04 but shifted toward higher temperatures (~60 K for M12 and ~80 K for M04) indicating a stronger localization degree [1,13,14]. Once again, the S-curve behavior in the PL peak position versus temperature data becomes more pronounced with increasing Al/In, as was displayed for sample M04 despite more indium (In) was incorporated into the layers than the other two samples [1].

Previously, we have investigated that the temperature-dependent of the InAlGaN band gap is somewhat different comparing with the temperature dependence of the GaN band gap (not shown here) [8]. Therefore, the studies of our quaternary structures of InAlGaN alloys over a wide temperature dependence of the PL peak position for the three InAlGaN samples were S-like shape due to the effect of localization of excitons in the density of states tails [8]. For the structures containing InAlGaN layers, the localization energy of excitons is defined as the deviation of the experimental temperature dependence of the InAlGaN-related PL peak positions at low temperature regions [8]. To study the exciton localization effects in the InAlGaN samples, we use the modified Bose–Einstein expression based on the band-tail-filling model, which takes the exciton localization effect into account [16–19]:

$$E_g(T) = E_B - a_B \times \left\{1 + \frac{2}{\left[\exp\left(\frac{\Theta_B}{T}\right) - 1\right]}\right\} - \frac{\sigma_E^2}{k_B T} \quad (1)$$

where $E_B = E_0 + a_B$ (E_0 is the band gap at 0 K), k_B is the Boltzmann constant, a_B is the magnitude of the limiting slope of the corresponding $E_g(T)$ curve attributed to the strength of the electron/exciton-phonon interaction, $\Theta_B = \hbar\omega_{eff}/k_B$ is the phonon temperature associated with the single ('phantom') oscillator under consideration corresponding to the average phonon temperature. The redshift of PL peak energy with decreasing temperature is due to statistical alloy broadening of the PL emission, and is given by $\sigma_E^2/k_B T$, where σ_E is defined to be close to the localization energy due to the potential fluctuations [20]. By fitting Eq. (1) (shown in Fig. 2b) to the appropriate range of temperature, it is noted that this modified model is based on Gaussian distribution of localized states and only valid above certain temperature, then the estimated values of E_B, a_B, Θ_B, and σ_E are obtained and listed in Table 1 with the

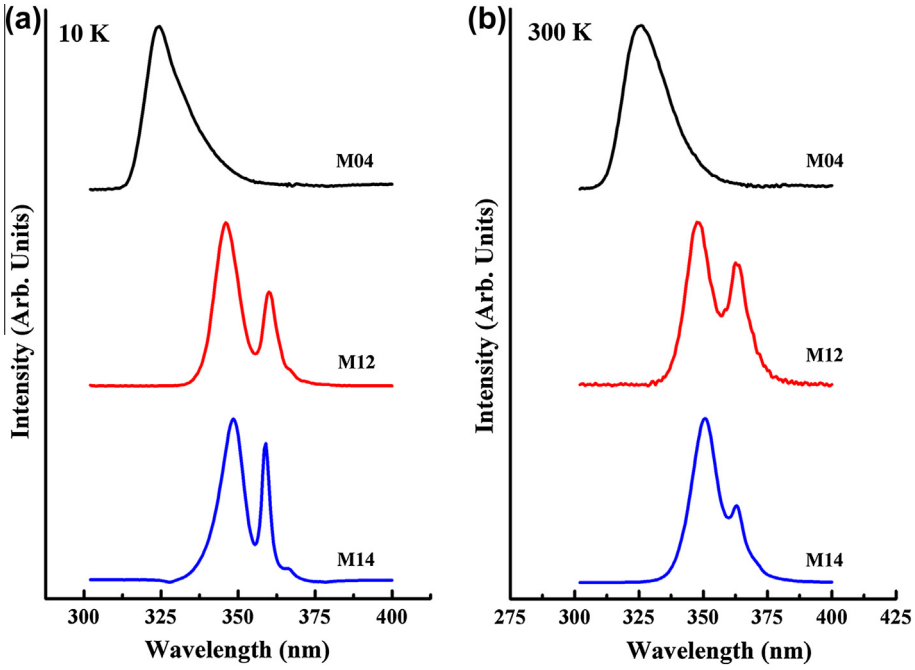

Fig. 1. Measurements of the PL spectra for the three quaternary InAlGaN samples, namely M14, M12, and M04 as labeled in (a) for 10 K, and (b) for 300 K, respectively were made under the same excitation conditions. As shown in (b), the short-wavelength PL signal has been previously assigned to be the InAlGaN-based transition, and the GaN-related features appearing on the right side of the InAlGaN-based PL peaks are all just about located at 364 nm for the samples of M14 and M12, respectively.

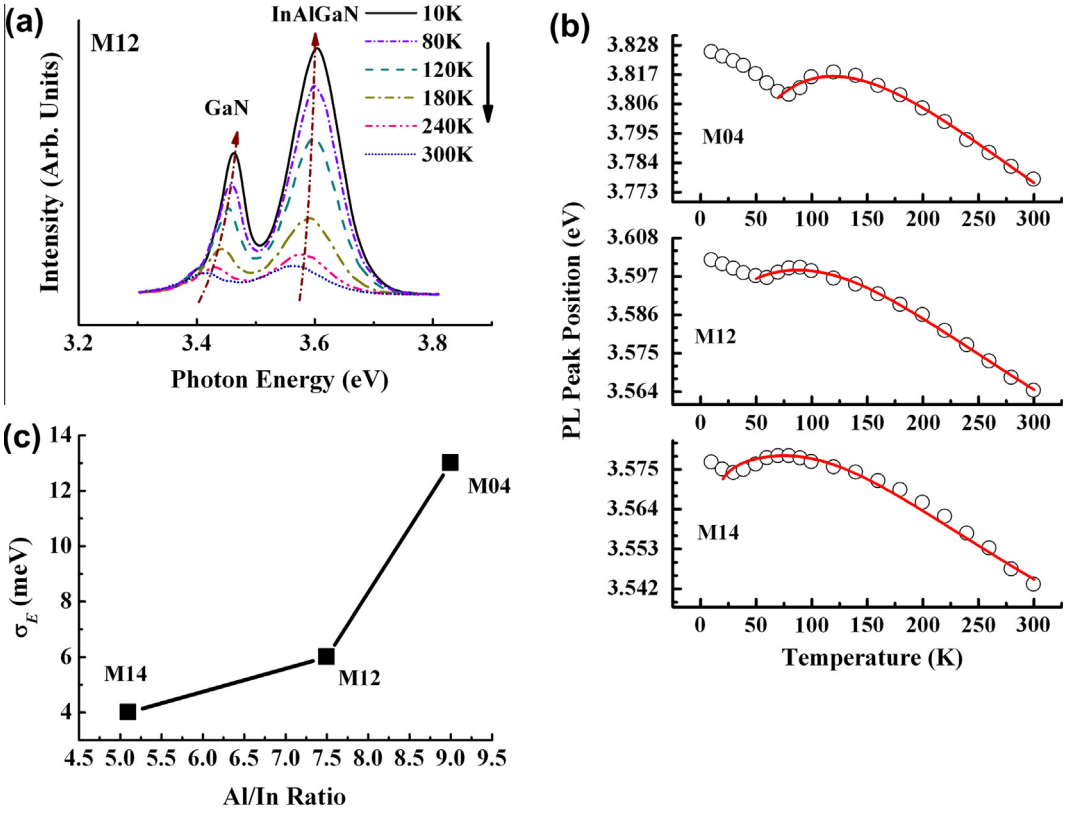

Fig. 2. The typical PL spectra of sample M12 at several different temperatures from 10 to 300 K is shown in (a), while the PL peak position (open circles) as a function of temperature are shown in (b), respectively. The solid lines are least squares fit to Eq. (1). The σ_E (closed squares) as a function of the Al/In ratio is shown in (c).

Table 1
With the representative error bar, values of the parameters E_B, a_B, Θ_B, and σ_E are obtained from a fit to Eq. (1) while the σ_s, and lattice constant c are calculated by Eq. (3), respectively.

Sample number	M14	M12	M04
E_B (eV)	3.58 ± 0.01	3.60 ± 0.01	3.84 ± 0.01
a_B (meV)	82 ± 2	94 ± 2	156 ± 2
Θ_B (K)	450 ± 25	480 ± 25	530 ± 25
σ_E (meV)	4 ± 1	6 ± 1	13 ± 1
σ_s (GPa)	−1.307 ± 0.001	−0.961 ± 0.001	−0.616 ± 0.001
Lattice constant c (Å)	5.191 ± 0.001	5.189 ± 0.001	5.188 ± 0.001

representative error bar [16–19]. For band gaps, temperature variations are due to both lattice constant difference and interactions with relevant acoustic and optical phonons. From the previous published literature, the presence of higher a_B could imply the strong electron/exciton-phonon interaction in InAlGaN sample enhanced by alloy disorder which might lead to a higher value of Θ_B [16]. Currently, the strength of the electron/exciton-phonon interaction for the case of higher Al/In ratio sample is larger than those of the lower Al/In ratio samples, the experimental evidence of larger values of a_B and σ_E might suggest a general characteristic of the crystals with higher Al/In ratio structure of InAlGaN. From the results of Table 1, σ_E varies in the range of 4 ± 1 to 13 ± 1 meV as the a_B increases from 82 ± 2 to 156 ± 2 meV, and the Θ_B increases from 450 ± 25 to 530 ± 25 K; those obtained values are similar to the previous report by James et al. and the above evidence may also be related to a strong effect of compositional fluctuation in higher Al/In ratio of InAlGaN layers, then the σ_E (closed squares) as a function of the Al/In ratio is shown in Fig. 2c [6,16].

As has been discussed, the PL spectra of our InAlGaN samples were dominated by the localized exciton emission which was induced by the potential fluctuations due to the alloy disordering or defects. The temperature-dependent PL measurements have performed to study the exciton localization effects and expect the PL intensities in all samples decrease with increasing temperature. The Arrhenius plots of integrated PL intensity (opened triangles) as a function of the temperature for all samples are displayed in Fig. 3, and the solid lines are the least squares fit of the data following the equation:

$$I_{PL}(T) = \left[1 + A\exp\left(\frac{E_a}{k_B T}\right)\right] \quad (2)$$

where E_a is the activation energy, A is a fitting constant, and k_B is the Boltzmann constant [2]. The fitted values of E_a are 0.032 ± 0.001 meV for M14, 0.018 ± 0.001 meV for M12, and 0.016 ± 0.001 meV for M04, respectively. In general, the measured activation energy can be regarded as a measure of the exciton localization effect in the alloys [2]. Consequently, it reflects the alloy uniformity or the degree of free from defects. The experimental results imply that E_a decreases with the increased Al/In ratio indicates that the random alloy disordering is increased with the increase of the Al/In ratio in our InAlGaN samples.

In order to consider the observed temperature-dependent PL properties with the material structure, we might have to analyze the effect of the incorporation of Al or In in the lattice and take into account that the InAlGaN layer is under compressive or tensile stress depending on its composition. Fig. 4 shows the (002) θ–2θ HRXRD patterns for the three InAlGaN samples with different Al/In ratios, while the peaks at around 34.5° originate from the underlying GaN layers, and all InAlGaN peaks locate at the right side of the GaN peaks [21]. The alloy system of In–Al–Ga–N samples with the Al/In ratio of around 4.7, which are lattice matched to the underlying GaN layer, exhibited the better structural properties, so the InAlGaN peak is close to the GaN peak observed for M14

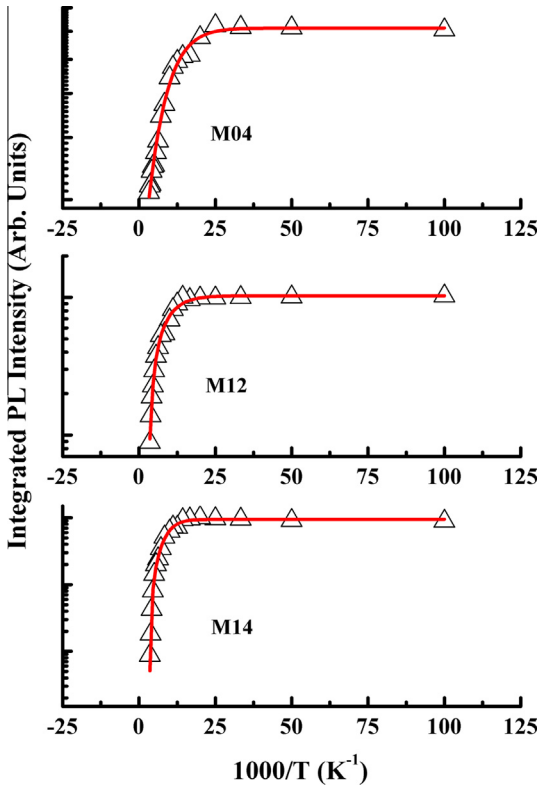

Fig. 3. The Arrhenius plots of integrated PL intensity (opened triangles) as a function of the temperature for the three samples, M14, M12, and M04 are shown here, respectively and the solid lines are the least squares fit to Eq. (2).

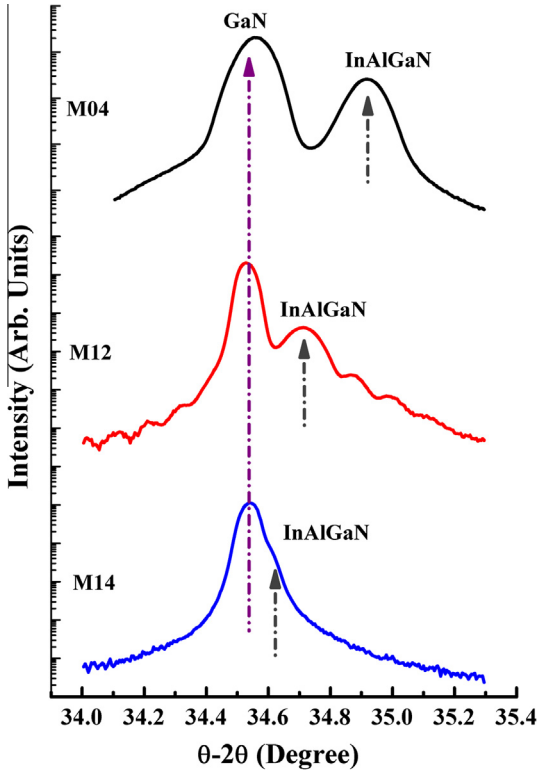

Fig. 4. HRXRD θ–2θ scan for the three InAlGaN samples with different Al/In ratios, while the peaks at (002) originate from the underlying GaN layers, and all InAlGaN peaks locate at the right side of the GaN peaks.

in Fig. 4 [11]. Additionally, Jiang and Lin have attributed the residual defects in the InAlGaN epilayer to the alloy compositional fluctuation (ACF), contributed by unfinished substitutions of Ga atoms that introduced point defects leading to non-uniformity of the quaternary alloys and the InAlGaN material system because mixing of In, Al and Ga atoms occurs on one of the sublattices [17]. Furthermore, we precisely investigate the residual stress in InAlGaN samples by analyzing the (002) peaks in HRXRD spectra. To derive the stress σ_s in InAlGaN samples, the following formula is used [22–24]:

$$\sigma_s = \frac{2c_{13}^2 - c_{33}(c_{11}+c_{12})}{2c_{13}} \times \frac{c - c_0}{c_0} \quad (3)$$

where c_{ij} $(i,j = 1,2,3)$ stands for the elastic constants in different orientation, c_0 is the lattice constant of GaN (5.185 Å), and c is the lattice constant of our InAlGaN sample which can be calculated by $c = 2d_{002} = \lambda/\sin\theta$ (λ: X-ray wavelength and θ: Bragg diffraction angle) [22–24]. Then, the stress σ_s in InAlGaN samples can be obtained by substituting the value of c_{ij} $(i, j = 1, 2, 3)$ in Eq. (3) with c_{11} = 374 GPa, c_{12} = 106 GPa, c_{13} = 70 GPa, and c_{33} = 379 GPa, respectively and presented in Table 1 with the representative error bar [22–24]. The σ_s (closed triangles) as a function of the Al/In ratio is shown in Fig. 5a, however the negative sign indicates the InAlGaN samples undergo the compressive stress and the residual stress of the InAlGaN samples has been reduced as the increasing of Al/In ratio [22–24]. Probably, with the increasing of Al/In ratio, the decreased compressive stress would be attributed to the increased tensile stress formed by Al atoms incorporated. Therefore, by further increasing the Al/In ratio, the tensile stress becomes stronger and eventually exceeds the compressive stress and leads to a change

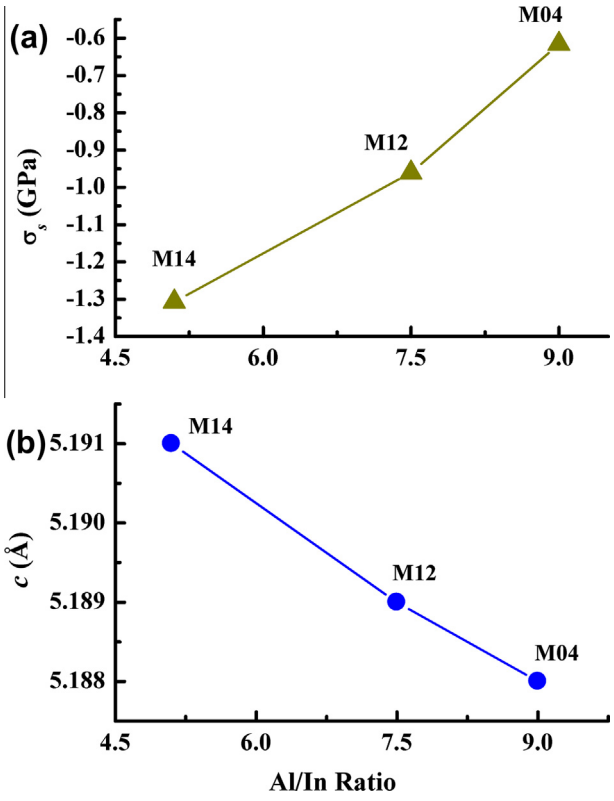

Fig. 5. As shown in (a), the σ_s (closed triangles) as a function of the Al/In ratio is shown here and the negative sign indicates the InAlGaN samples undergo the compressive stress and the residual stress of the InAlGaN samples has been reduced as the increasing of Al/In ratio. As shown in (b), due to the lattice mismatch induced strain, the lattice constant c decreases linearly from 5.191 ± 0.001 to 5.188 ± 0.001 Å with the increase of Al/In ratio, and the c (closed circles) as a function of the Al/In ratio is shown here.

in the direction of stress. Then, the results of residual stress are quite confirmed as the increasing of Al/In ratio, the Al-rich InAlGaN diffraction peaks appear on the right side of GaN peak. Furthermore, the increasing distance between the GaN and Al-rich InAlGaN (002) peaks with increasing Al/In indicates a stronger stress in M04 to be the largest one, demonstrating the biggest lattice mismatch and stress existing in M04 among the three samples [25]. Due to the lattice mismatch induced strain, the lattice constant *c* decreases linearly from 5.191 ± 0.001 to 5.188 ± 0.001 Å with the increase of Al/In ratio (listed in Table 1), and the *c* (closed circles) as a function of the Al/In ratio is shown in Fig. 5b. Then, HRXRD confirms the temperature dependence PL analysis where the sample with higher Al/In ratio in this study does not reveal considerable variation in residual stress but generates more localization effects.

4. Conclusions

Quaternary alloys in the structure containing thin InAlGaN film separated by GaN layer with different Al/In ratios have been investigated by PL techniques. Temperature dependence of the PL peak energy in the range of 10–300 K exhibits S-shaped behavior and becomes more pronounced with increasing Al/In ratio. The localization energy would increase almost linearly with decreasing emission wavelength in the spectral region of 300–400 nm. Furthermore, the higher Al/In InAlGaN samples contributing to the larger values of the localization energy of excitons which are confirmed to be related with the strength of the electron/exciton-phonon interaction as well as the stress. As a result, it is interesting to notice that photoluminescence property is more strongly influenced by the fact of Al/In in the In–Al–Ga–N alloy system.

Acknowledgements

The authors would like to acknowledge the support of the National Science Council Project NSC102-2221-E-272-006 and NSC99-2112-M-236-001-MY3. The work at National Taiwan University was supported by NSC 98-2221-E-002-015-MY3 and NTU Excellent Research Project (10R80908 and 102R890954).

References

[1] K.B. Lee, P.J. Parbrook, T. Wang, F. Ranalli, T. Martin, R.S. Balmer, D.J. Wallis, J. Appl. Phys. 101 (2007) 053513.
[2] N. Nepal, K.B. Nam, J. Li, M.L. Nakarmi, J.Y. Lin, H.X. Jiang, Appl. Phys. Lett. 88 (2006) 261919.
[3] S. Nagarajan, Y.S. Lee, M.S. Kumar, O.H. Cha, C.H. Hong, E.K. Suh, J. Phys. D Appl. Phys. 41 (2008) 012001.
[4] H. Hirayama, J. Appl. Phys. 97 (2005) 091101.
[5] J.C. Zhang, Y.H. Zhu, T. Egawa, S. Sumiya, M. Miyoshi, M. Tanaka, Appl. Phys. Lett. 92 (2008) 191917.
[6] X.A. Cao, Y. Yang, Appl. Phys. Lett. 96 (2010) 151109.
[7] K. Kazlauskas, G. Tamulaitis, A. Zukauskas, M.A. Khan, J.W. Yang, J. Zhang, E. Kuokstis, G. Simin, M.S. Shur, R. Gaska, Appl. Phys. Lett. 82 (2003) 4501.
[8] S.Y. Hu, Y.C. Lee, Z.C. Feng, S.H. Yang, J. Alloys Comp. 509 (2011) 2300.
[9] H. Kang, S. Kandoor, S. Gupta, I. Ferguson, S.P. Guo, M. Pophristic, Phys. Stat. Sol. (c) 2 (2005) 2145.
[10] S.Y. Hu, Y.C. Lee, Z.C. Feng, S.H. Yang, J. Lumin. 132 (2012) 1037.
[11] T.N. Oder, J. Li, J.Y. Lin, H.X. Jiang, Appl. Phys. Lett. **77** (2000) 791.
[12] M.E. Aumer, S.L. LeBoeuf, F.G. McIntosh, S.M. Bedair, Appl. Phys. Lett. 75 (1999) 3315.
[13] E. Monroy, N. Gogneau, F. Enjalbert, F. Fossard, D. Jalabert, E. Bellet-Amalric, L.S. Dang, B. Daudin, J. Appl. Phys. 94 (2003) 3121.
[14] S. Fernández-Garrido, J. Pereiro, F. González-Posada, E. Muñoz, E. Calleja, A. Redondo-Cubero, R. Gago, J. Appl. Phys. 103 (2008) 046104.
[15] R.J. Potter, N. Balkan, J. Phys.-Condens. Mater. 16 (2004) S3387.
[16] G.R. James, A.W.R. Leitch, F. Omnès, M. Leroux, Semi Sci. Technol. 21 (2006) 744.
[17] H.X. Jiang, J.Y. Lin, Opt. Electron. Rev. 10 (2002) 271.
[18] S.O. Usov, A.F. Tsatsulnikov, V.V. Lundin, A.V. Sakharov, E.E. Zavarin, D.S. Sizov, M.A. Sinitsyn, N.N. Ledentsov, Semiconductors 42 (2008) 720.
[19] H.P.D. Schenk, M. Leroux, P. de Mierry, J. Appl. Phys. 88 (2000) 1525.
[20] J. Christen, D. Bimberg, Phys. Rev. B 42 (1990) 7213.
[21] S.Y. Hu, Y.C. Lee, Z.C. Feng, Y.H. Weng, J. Appl. Phys. 112 (2012) 063111.
[22] M.E. Aumer, S.F. LeBoeuf, S.M. Bedair, M. Smith, J.Y. Lin, H.X. Jiang, Appl. Phys. Lett. 77 (2000) 821.
[23] R. Hong, J. Huang, H. He, Z. Fan, J. Shao, Appl. Surf. Sci. 242 (2005) 346.
[24] A. Cros, A. Cantarero, N.T. Pelekanos, Georgakilas, J. Pomeroy, M. Kuball, Phys. Stat. Sol. 1674 (b) (2006) 243.
[25] J.S. Huang, X. Dong, X.D. Luo, D.B. Li, X.L. Liu, Z.Y. Xu, W.K. Ge, J. Crystal Growth 247 (2003) 84.